Lagrangian Simulation of Turbulent Particle Dispersion in Electrostatic Precipitators

Alfredo Soldati, Massimo Casal, Paolo Andreussi, and Sanjoy Banerjee
Dip. di Scienze e Tecnologie Chimiche, Università di Udine, Udine, Italy 33100

Industrial design of electrostatic precipitators is based on the transport theory developed by Deutsch (1922), which assumes that transverse turbulent mixing is effective enough to maintain the concentration profile uniform throughout the cross section (i.e., turbulent diffusivity is assumed infinite). To improve understanding of turbulent particle dispersion under the influence of electrostatic forces, a database on particle trajectories was first generated, based on the flow field from a direct numerical simulation of a plate-plate precipitator (Soldati et al., 1993). The effect of various parameters, such as particle size, charge and particle migration velocity, on dispersion and collection efficiency was investigated. Results show that particle concentration profiles are not uniform due to finite values of "turbulent diffusion" coefficient. The simulations indicate that the early stages of particle collection are controlled by particle migration velocity, while final stages are controlled by turbulence diffusion mechanisms.

Introduction

Electrostatic precipitation is widely employed to remove dust from industrial gas streams. The main application is to control the release of waste particles to the atmosphere, but it is also used to improve product quality and, in some cases, to collect valuable materials.

An electrostatic precipitator (ESP) is essentially a duct with vertical walls through which a gas bearing suspended particles is driven by a pressure gradient. Particles are transported by the turbulent gas stream and are driven toward a collecting surface by the electrostatic field maintained between the walls. In plate–plate precipitators, which are usually the second stage of a two-stage precipitator, a potential difference applied between the plates generates a uniform and constant electrostatic field. In this type of precipitator, sketched in Figure 1, charged particles are driven by a uniform and constant drift force toward the collecting plate.

The design of an ESP is based on knowledge of (or on reasonable assumptions regarding) particle transport. In the past, fundamental studies on particle transport have been carried out in several ways, beginning with the early model of Deutsch (1922). Using the analogy of a fabric filter (or equivalently, with the absorption of radiation by a slab), he postulated that the variation of particle concentration, dn, due to particle deposition at the wall over a differential length, dx, at a distance x from the entrance, would be related to several factors, namely, particle concentration at x, $n(x)$; the particle transverse migration velocity, w_e; the flow mean velocity, U_m; and the duct spacing, d. This ultimately leads to $dn(x) = -w_e/(U_m d)n(x)dx$. Integrating this last expression, and defining the dimensionless number $De = (w_e x)/(U_m d)$,

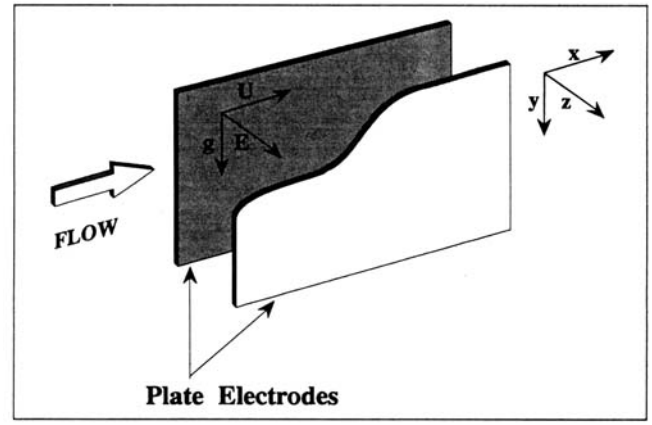

Figure 1. Plate–plate electrostatic precipitator.

Correspondence concerning this article should be addressed to A. Soldati.
Current address of S. Banerjee: Department of Chemical Engineering, University of California at Santa Barbara, Santa Barbara, CA 93106.

the Deutsch number, the collection efficiency, η may be calculated as

$$\eta = \frac{n(x)}{n(0)} = 1 - \exp[-De]. \tag{1}$$

The Deutsch number may represent the dimensionless distance covered by particles in the flow direction (Soldati et al., 1995a). The migration velocity is calculated by balancing the drag force and the Coulomb force acting on a particle. In the Stokes regime, it has the form:

$$w_e = \frac{q_p E}{3\pi d_p \mu}, \tag{2}$$

where q_p and d_p are particle charge and diameter, E is the modulus of the electrostatic field, and μ is fluid viscosity. This velocity is useful as a reference, but may not give the actual migration velocity of a particle, which must be determined by solving the equations for particle motion.

In Eq. 1, all the transport-related aspects for the particles are lumped into the Deutsch number, which represents an implicit model of turbulent transport based on the assumption that transverse turbulent mixing is so effective that it keeps particle concentration uniform over the cross section. The simplicity of Eq. 1 is one of the reasons justifying its broad use in ESP design. It is oversimplified, and empirical coefficients have to be used for actual design. Improvements in the Deutsch model were later suggested by Robinson (1967), who modified Eq. 1 to include erosion of deposited particles, and by Cooperman (1971 and 1977), who proposed a different method for calculating the net velocity of particles. However, both researchers based their correlations on Eq. 1.

More recently, new analyses, prompted by more stringent regulations regarding atmospheric emissions, have been performed to improve understanding of the basic precipitation mechanisms and to optimize ESP design. One of the approaches followed is based on the use of an advection/diffusion equation (ADE) by assuming a Fickian form for the turbulent dispersion mechanism. Turbulent diffusion is postulated as isotropic and homogeneous and the ADE is solved for the unknown value of the turbulent dispersion coefficient by fitting data. Williams and Jackson (1962) and later Leonard et al. (1980) studied the effect of finite diffusivity by solving the two-dimensional (2-D) ADE. In particular, the model by Leonard et al. (1980, 1982) relies on a tunable, isotropic, and uniform turbulent diffusion coefficient, D, which they expressed through the electric Péclet number defined as $w_e d/D$. This approach, and especially the conclusions of the article, were severely criticized by Cooperman (1982)—in particular, the *a posteriori* determination of unrealistically low turbulent diffusion coefficients, which raised the collection efficiency.

In order to understand particle dispersion mechanisms, knowledge of the turbulent flow field is required. In recent years, direct numerical simulation (DNS) has been used as a powerful tool to fully simulate three-dimensional (3-D) time-fluctuating turbulent flow fields (Kim et al., 1987; Lam and Banerjee, 1992; Papavassiliou and Hanratty, 1995, among others). In previous articles (Soldati et al., 1993 and 1995b), this method was also applied to simulate particle dispersion in ESPs. The advantage of DNS is that the solution of the Navier–Stokes equations is free from empirical models, or closure laws, that affect methods based on averaging or filtering (e.g., $k-\epsilon$ methods). The 3-D time-varying turbulent field obtained by DNS is accurate down to the dissipation scales of motion if sufficient spatial and temporal resolution is used. Numerical experiments performed by DNS are therefore becoming a means of investigating turbulence structure and turbulent transport mechanisms, and have proved to be of help in focusing and refining experimental investigations. The present limitation of DNS is due to the size of the available supercomputers, but with massively parallel machines, problems at scales of interest to industry and Reynolds numbers are becoming increasingly feasible.

The approach followed in this work is therefore more direct when compared to the works by Leonard et al. (1980, 1982), and is based on a DNS of turbulent channel flow to determine turbulent particle transport parameters and collection efficiency directly from particle trajectories. In other words, the behavior of swarms of particles of different diameters and diffusivity was examined tracking each particle by solving its equation of motion. This made it possible to determine the effects of inertia and drift velocity on transport parameters and on the collection efficiency of the precipitator.

Transverse dispersion coefficients were determined assuming homogeneous turbulent diffusion (Taylor, 1921), which, for the duct flow under investigation, may be acceptable in the central region of the duct, where the fluid turbulence is relatively homogeneous. It was found that particle dispersion varies with particle size and electric charge, as expected. On the basis of these data, a correlation for turbulent particle dispersion in ESPs was set up and assessed by comparison against previous experiments and theories.

Since ESP efficiencies should be very high (close to unity), improvement of their design is of considerable interest and requires a clearer understanding of turbulent particle transport and its impact on deposition rates. From numerical simulation of particle collection efficiency, the early stages of deposition appear to be controlled by the drift velocity, while bulk turbulent dispersion mechanisms seem to control the final stages. It appears that these effects can be captured by using a 2-D ADE of the form used by Leonard et al. (1980). It has been demonstrated that if diffusion coefficients and migration velocity measured from the present simulations are used, the ADE underpredicts the data on collection efficiency by about 1 to 2%. This may be caused by the adoption of a uniform transverse turbulent diffusion coefficient that overestimates turbulent transport in the wall layer.

Computational Method

The flow field in ESPs is 3-D, time-dependent, and turbulent, but characterized by a rather low Reynolds number. Because of this, DNS may be used to obtain a flow-field database. Once the flow field is known in detail, particles may be released and followed under the action of the flow field and electrostatic forces. The solution of the fluid-dynamic problem was described in a previous article (Soldati et al., 1993) that simulated the turbulent flow of air in a duct at a Reynolds number of 5980 based on the hydraulic diame-

ter and the mean velocity. Some aspects of the technique adopted to calculate the flow field are briefly reviewed here.

Flow field

The flow field of a pressure-driven fully turbulent flow in a duct with parallel vertical walls (Figure 1) was computed by solving the time-dependent 3-D Navier–Stokes equations in the following dimensionless form:

$$\frac{\partial u_i}{\partial t} + u_j \frac{\partial u_i}{\partial x_j} = \delta_{1i} + \frac{1}{Re} \frac{\partial^2 u_i}{\partial x_j \partial x_j} - \frac{\partial p}{\partial x_i}, \tag{3}$$

where u_i are the velocity components; p is the fluctuating kinematic pressure (pressure divided by density); and δ_{1i} represents the mean kinematic pressure gradient that drives the flow. Equation 3 was made dimensionless by using the channel half-width, h, and the shear velocity, defined as:

$$u_\tau = \sqrt{\frac{\tau_w}{\rho}}, \tag{4}$$

where τ_w is the shear stress at the wall; ρ the fluid density.

In dimensionless units, the size of the computational domain is $4\pi \times 2\pi \times 2$. For air flowing at a mean velocity of 1.16 m/s, a value typical for ESPs, the dimension of the computational domain would be $25 \times 12 \times 4$ cm. The solution of Eq. 3 is obtained by using a pseudospectral method (Kim et al., 1987; Lam and Banerjee, 1992; Soldati et al., 1993) and is based on the decomposition of the flow variables in Fourier series in the x and y directions and in Chebyshev polynomials in the z-direction. Thus, the velocity field has the form:

$$u(x,y,z,t) = \sum_{k_1} \sum_{k_2} \sum_{k_3} \hat{u}(k_1,k_2,k_3,t) \times \exp[i(k_1 x + k_2 y)] \cos(k_3 \cos^{-1} z), \tag{5}$$

where $\hat{u}(k_1,k_2,k_3,t)$ is the velocity field in the spectral domain, and k_1, k_2, k_3 are the wave numbers. The fluid velocity is subject to rigid boundary conditions at the walls of the duct, and periodic boundary conditions are imposed in the x and y directions. If wall variables, identified by the superscript $+$, are used, that is, variables made dimensionless by u_τ and by the fluid kinematic viscosity, ν, the channel is 216 wall units wide, and the periodicity lengths are 1,357 and 676 in the x and y directions, respectively. The periodicity lengths are more than two times the spatial correlation in both directions, which ensures the development of turbulent channel flow. The time advancement was provided by a two-level Adams–Bashforth method for the convective terms and by an implicit Crank–Nicolson method for the diffusive terms. The time step was $\Delta t^+ = 0.1$. Parameters characterizing the flow field are shown in Table 1.

The statistics of the flow field were compared with experimental data in an earlier work (Soldati et al., 1993). However, to help in later discussion, mean velocity and rms values are shown in Figures 2a and 2b. The mean velocity profile is a typical turbulent flow profile and differs from those used by Leonard et al. (1980), Kihm (1987), and Tsai (1991), who assumed a uniform plug flow profile to develop their models. In Figure 2b, turbulence intensities u', v', w' are shown: turbulence intensity reaches the highest value near the wall in the x and y directions, while in the z-direction the profile is nearly uniform for most of the channel except for the region very near the walls.

Table 1. Parameters Relative to the Simulation of the Turbulent Flow Fields

Reynolds number	$\mathrm{Re} = \frac{U_m 4h}{\nu} = 5{,}980$
Shear Reynolds number	$\mathrm{Re}_\tau = \frac{u_\tau h}{\nu} = 108$
Dimensionless mean velocity	$U_m/u_\tau = 13.7$
Mean velocity	$U_m = 1.16$ m/s
Center-line velocity	$U_c = 1.40$ m/s
Fluid density	$\rho = 1.29$ kg/m^3
Fluid kinematic viscosity	$\nu = 1.57 \cdot 10^{-5}$ m^2/s
Fourier modes (x)	$N_x = 64$
Fourier modes (y)	$N_y = 64$
Chebyshev modes (z)	$N_z = 65$
Time step	$\Delta t^+ = \Delta t\, u_\tau^2/\nu = 0.108$

Particle tracking

Using DNS databases to simulate transport of particles in various situations has been the subject of much recent work. Measurements of particle dispersion in flow fields generated by DNS have been performed by Ounis et al. (1989), who quantified the dispersion of Brownian particles in vertical turbulent channel flow; by Squires and Eaton (1991) for homogeneous and isotropic turbulence flow; by Kontomaris and Hanratty (1994) for turbulent channel flow; and by Chen and McLaughlin (1995), who studied aerosol deposition rates in vertical ducts.

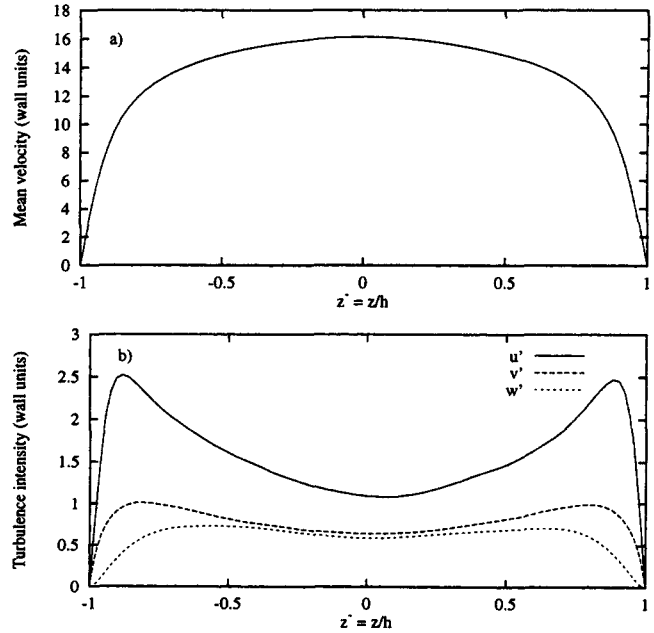

Figure 2. Turbulence in the duct: (a) mean velocity profile; (b) turbulence intensity.

In this work, a DNS database was used to simulate turbulent transport of particles subject to electrostatic body forces in plate–plate ESPs. The main objectives were, first, to obtain dispersion characteristics for different particle sizes and different drift velocities in order to set up a model for a macroscopic turbulent diffusion coefficient, and second, to assess the influence of macroscopic transport properties on collection efficiency in ESPs.

Particle dispersion characteristics depend on particle drift velocity, expressed by the particle migration velocity, w_e, and on particle inertia, characterized by the particle relaxation time, τ_p (the Stokesian response time), defined by

$$\tau_p = \frac{d_p^2 \rho_p}{18\mu}, \tag{6}$$

where ρ_p is particle density. Note that τ_p defined in this way is only an indicator of particle response for relative velocities higher than those in creeping flow. In the present simulations, particles have been tracked individually by numerically solving the equation of motion, which includes the electrostatic force, gravity, and fluid drag. Since in the present simulation the particles are meant to correspond to an experiment with an aerosol of oleic acid, the density is 900 kg/m^3, as in the work by Leonard et al. (1982) and Self et al. (1987). Other forces acting on the particle, such as hydrostatic force, added mass force, lift force, Magnus effect, and Basset history force, are negligible (orders of magnitude smaller than the three effects considered) for the case investigated. Also, particles are assumed to be rigid and pointwise, and at concentrations low enough for particle–particle interaction due to either inertial force or electrostatic repulsion to be negligible. The vectorial equation of motion made dimensionless using scales characteristic of the wall region, that is, the shear velocity and the fluid kinematic viscosity, is

$$\frac{dv^+}{dt^+} = -\frac{v^+ - u^+}{\tau_p^+} f(Re_p) + \frac{\rho - \rho_p}{\rho} g^+ + \frac{1}{Fr_p^2} e, \tag{7}$$

where v^+ is particle velocity, g^+ is the dimensionless gravity vector, e is the electric field unit vector, and Fr_p is the dimensionless electric-Froude number (Soldati et al., 1995a), defined as

$$Fr_p = \sqrt{\frac{m_p u_\tau^3}{q_p \nu E}}. \tag{8}$$

In Eq. 7, $f(Re_p)$ is a function of the particle Reynolds number, Re_p, which depends on the fluid dynamic drag law adopted. In this work, we adopted the form proposed by Rowe and Henwood (1962), that is,

$$f(Re_p) = 1 + 0.15 Re_p^{0.697}. \tag{9}$$

The trajectory of each particle was calculated integrating Eq. 7 by an explicit method. The velocity of the fluid at each particle position was calculated directly from the triple sums of the spectral coefficients. This method is accurate, but its cost in terms of computer time rapidly becomes prohibitive because of the number of particles tracked (Yeung and Pope, 1988). For the number of particles used in the present simulation (4,000), the computer time is comparable to that required for other types of interpolations. The initial velocities of the particles were set equal to the fluid velocity at each particle location.

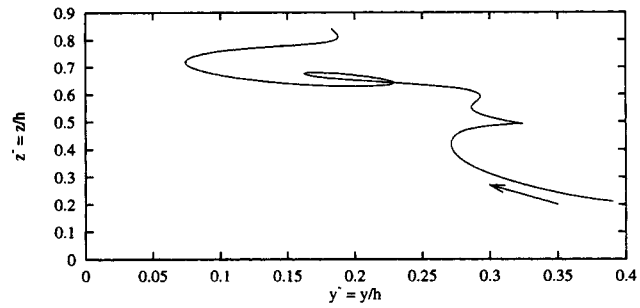

Figure 3. Example of the trajectory of a particle in the y-z plane.

Using this simulation of particle motion, a deterministic description of the dispersion field may be computed since the trajectory of all particles is available. In Figure 3, the trajectory in the $y - z$ plane of an 8-μm particle with a drift velocity of $w_e = 10$ cm/s is shown to indicate the type of results obtained from the integration of Eq. 7. The effect of the turbulence structures is clear and is strong enough to make the particle follow a complex, hard-to-predict path.

Turbulent Diffusion

Theory of dispersion in homogeneous turbulence

In his work on diffusion in homogeneous turbulence, Taylor (1921) related the turbulent diffusion coefficient, $D(t)$, to the rate of growth of variance (RGV) as

$$D(t) = \frac{d\langle z(t)^2 \rangle}{dt}, \tag{10}$$

where $\langle z(t)^2 \rangle$ is the variance of the displacement distribution, defined as:

$$\langle z(t)^2 \rangle = \frac{1}{N(t)} \sum_{n=1}^{N(t)} \left[z_n(t) - \frac{1}{N(t)} \sum_{n=1}^{N(t)} z_n(t) \right]^2, \tag{11}$$

in which $N(t)$ is the number of realizations. Thus, turbulent diffusivity is a time-dependent quantity that reaches a constant value at large diffusion times. Indeed, particle trajectories lose their initial correlation for developed turbulent flows when $t \to \infty$, and the probability distribution of the displacement function tends to become normal or Gaussian (Batchelor, 1957). It follows that the diffusion coefficient, D, can be expressed as the limit of $D(t)$ for $t \to \infty$:

$$D = \lim_{t \to \infty} D(t) = \lim_{t \to \infty} \frac{d\langle z^2 \rangle}{dt}. \tag{12}$$

Squires and Eaton (1991) and by Wang and Stock (1993), among others, have used this approach to characterize particle dispersion in homogeneous turbulence. This approach was also applied to different nonhomogeneous turbulent flows, for instance in mixing layers, by Chein and Chung (1988), Crowe et al. (1988), and Aggarwal et al. (1994), and by Ounis et al. (1991) for turbulent channel flows, to quantify the dispersion of Brownian particles; by Kontomaris and Hanratty (1994), to investigate the effect of molecular diffusivity on the diffusion of a scalar property; and by Papavassiliou and Hanratty (1995), to describe the turbulent transport of heat from a wall. In general, Eq. 12 may be of some use as long as the turbulence is far from the boundaries and relatively homogeneous—clearly not the case for channel turbulence in the region close to the walls. However, Eq. 12 may be representative of the phenomenon in the central region of the duct.

Particle dispersion in electrostatic precipitators

Transport of particles in ESPs is controlled by mean flow convection in the direction of the stream (x), by electrostatic drift in the wall-normal direction (z), by gravity (a small effect) in the spanwise direction y, and by turbulent dispersion in all three directions. Dispersion effects in the x (streamwise) and y (spanwise) directions do not appear as relevant to particle-collection efficiency as those in the transverse direction (Leonard et al., 1980). Therefore, in this work, only the turbulent dispersion in the wall-normal direction is examined.

Transverse turbulent dispersion is related to the intensity of turbulent fluctuations in the z-direction (see Figure 2b), which is almost uniform in the central region of the duct and goes to zero at the wall. Similar behavior can be expected from the turbulent dispersion coefficient, which should go to zero in the wall layer. For simplicity and with an eye to practical use of the results, the theory of diffusion in homogeneous turbulence will be applied to evaluate the diffusion coefficient in the central, nearly homogeneous region, and this coefficient will be assumed uniform for the whole width of the duct. Clearly, this leads to overestimation of the effects of transverse dispersion on particle transport in the wall layer.

In order to use Eq. 12, particles should remain in the central region of the duct long enough for the distribution of their displacement to become Gaussian, as discussed by Kontomaris and Hanratty (1994) and by Soldati et al. (1995b). To ensure this, particles were homogeneously distributed in an x-y plane, parallel to the wall, 0.5 h (one-half of the channel half-width) away from the noncollecting wall. In ESPs, particle size ranges from less than one μm up to tens of μm. In the present work, turbulent dispersion of particles of size 4, 8, 16 and 24 μm were simulated. Dimensionless and dimensional parameters characterizing the particles tracked are reported in Table 2. Inertia and drift velocity were both varied in order to examine their effect on dispersion characteristics. Drift velocity is related to particle charge, which, in the presence of free ions (as in the charging section of a precipitator), is a function of the applied electrostatic field via the equation

$$q_p = 3\pi \frac{\epsilon}{\epsilon + 2} \epsilon_0 E d_p^2, \tag{13}$$

where ϵ_0 is the permittivity of vacuum and ϵ is the dielectric constant of the aerosol particle, which for oleic acid equals 2.

Sixteen different swarms of particles characterized by the parameters of Table 2 were tracked. Each swarm comprised 1,000 particles, a number large enough to obtain meaningful statistics and low enough to save computer time. Previous results (Soldati et al., 1995b) showed no difference when calculating the variance of the displacement distribution using swarms of 600 or 900 particles.

In Figure 4, the displacement distribution at two different dimensionless times ($t^+ = 16$ and $t^+ = 32$) is reported for particles having diameters of 4, 8, 16 and 24 μm and a migration velocity of 10 cm/s. Symbols represent computed values, while lines represent a fitted Gaussian probability function. The distribution in Figure 4 were calculated after a time longer than the particle Lagrangian autocorrelation time. The Gaussian distribution has the following form:

$$N(z) = \frac{k}{\sqrt{\langle z(t)^2 \rangle 2\pi}} \exp\left[-\frac{z(t)^2}{2\langle z(t)^2 \rangle} \right], \tag{14}$$

where k is a normalization constant equal, for all the cases, to 0.05. From data fitted with a Gaussian distribution, as in Figure 4, it is possible to estimate $\langle z(t)^2 \rangle$. The results show that particle displacement distributions are well fitted by a Gaussian distribution for the central region of the duct.

Effect of Inertia on Particle Dispersion. To examine the effect of inertia, $\langle z(t)^2 \rangle$ was calculated for different particle sizes. Furthermore, to have a reference value, turbulent dis-

Table 2. Parameters Relative to the Simulation of Particle Dispersion

Fr_p	w_e (cm/s)	E (V/m)	q (C)	Fr_p	w_e (cm/s)	E (V/m)	q (C)
	(*a*) $\tau_p^+ = 0.018$ ($d_p = 4$ μm)				(*b*) $\tau_p^+ = 0.072$ ($d_p = 8$ μm)		
0.18	5	2.39×10^5	1.60×10^{-16}	0.35	5	1.70×10^5	4.54×10^{-16}
0.125	10	3.40×10^5	2.27×10^{-16}	0.25	10	2.39×10^5	6.38×10^{-16}
0.091	20	4.80×10^5	3.20×10^{-16}	0.18	20	3.39×10^5	9.05×10^{-16}
0.07	30	5.87×10^5	3.92×10^{-16}	0.14	30	4.15×10^5	1.11×10^{-15}
	(*c*) $\tau_p^+ = 0.286$ ($d_p = 16$ μm)				(*d*) $\tau_p^+ = 0.645$ ($d_p = 24$ μm)		
0.71	5	1.20×10^5	1.28×10^{-15}	1.08	5	9.70×10^4	2.33×10^{-15}
0.50	10	1.70×10^5	1.82×10^{-15}	0.76	10	1.37×10^5	3.29×10^{-15}
0.36	20	2.39×10^5	2.55×10^{-15}	0.54	20	1.93×10^5	4.64×10^{-15}
0.29	30	2.93×10^5	3.13×10^{-15}	0.44	30	2.39×10^5	5.74×10^{-15}

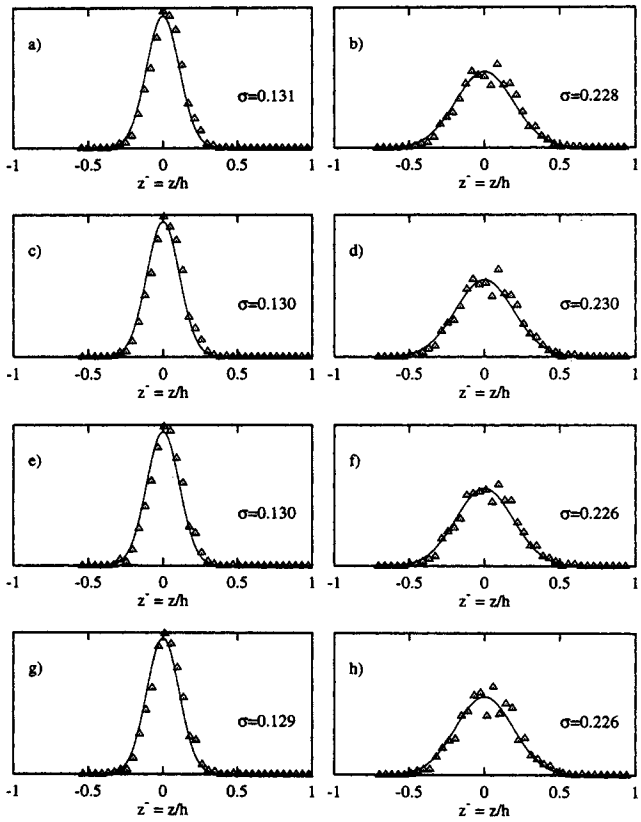

Figure 4. Distribution of the displacement probability.

$w_e = 10$ cm/s: (a) $d_p = 4$ μm, $t^+ = 16$; (b) $d_p = 4$ μm, $t^+ = 32$; (c) $d_p = 8$ μm, $t^+ = 16$; (d) $d_p = 8$ μm, $t^+ = 32$; (e) $d_p = 16$ μm, $t^+ = 16$; (f) $d_p = 16$ μm, $t^+ = 32$; (g) $d_p = 24$ μm, $t^+ = 16$; (h) $d_p = 24$ μm, $t^+ = 32$.

persion of fluid parcels was calculated using an inertialess and chargeless tracer.

In Figure 5a, the profiles of $\langle z(t)^2 \rangle$ for fluid and neutral particles are presented as a function of the dimensionless time. After a certain time, related to the particle Lagrangian autocorrelation time, the slope of the displacement variance becomes constant. This particular instant can be considered, with good approximation, to be identical for each curve and larger than 30 dimensionless time units. Indeed, all $\langle z(t)^2 \rangle$ profiles differ very little from each other, with inertia playing a minor role in the dispersion process. Figure 5b shows results obtained from applying Eq. 12 to data of Figure 5a. The values of the diffusivity for particles, D_p, were made dimensionless with the diffusivity of fluid parcels, D_f, thus defining a particle turbulent Schmidt number as

$$Sc_t = \frac{D_p(t)}{D_f(t)}. \qquad (15)$$

The asymptotic value of Sc_t is slightly larger for particles with smaller inertia, as expected, though the influence of inertia is relatively small for the range of particle dimensions examined. Inertia acts both ways, that is, increasing inertia leads to a decrease in the velocity fluctuations experienced by the particle, thus decreasing Sc_t. On the other hand, a similar incremental increase in inertia corresponds to an increase in

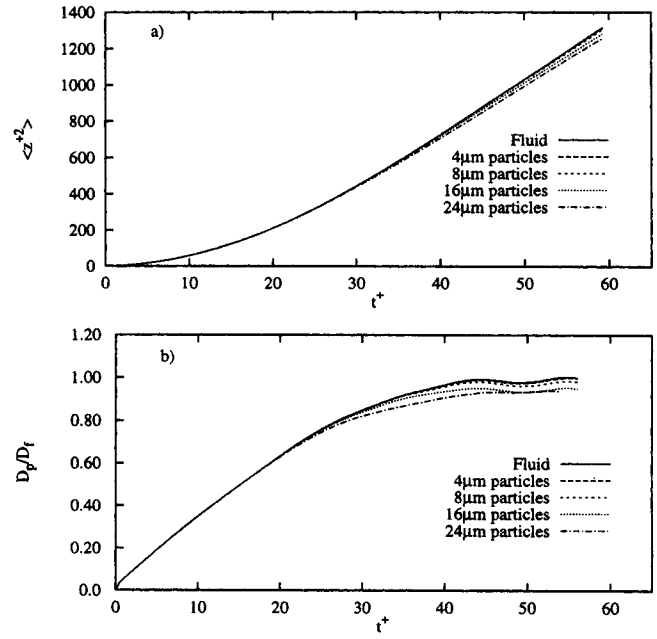

Figure 5. Effect of inertia on dispersion of neutral particles: (a) effect on $\langle z(t)^2 \rangle$; (b) effect on turbulent diffusivity.

the particle Lagrangian correlation time, which tends to increase turbulent dispersion. The present results for nonhomogeneous turbulence are therefore in line with the trends found for homogeneous and isotropic turbulence (see Reeks, 1977; Pismen and Nir, 1978; and Reynolds, 1995, for theoretical work, and Squires and Eaton, 1991, for numerical work).

Effect of Migration Velocity on Particle Dispersion. The other variable that influences turbulent diffusion is migration velocity, which is responsible for the "crossing trajectories effect" (Yudine, 1959). The action of the electrostatic field forces the particle to move through its immediate neighborhood. Therefore, we might expect that a particle with higher migration velocity will disperse less, since it is less affected by the surrounding fluid turbulence.

In Figure 6, the curves show the variance of the displacement distribution for the particles for all the different migration velocities. The time necessary to reach a Gaussian distribution is much shorter if a body force acts on particles. This effect may be seen by examining the four plots in sequence. As expected, the stronger the body force, the less particles disperse. It is clear that the drift velocity has a much stronger influence on particle dispersion compared to the effects of particle inertia (Meek and Jones, 1973; Nir and Pismen, 1979; Squires and Eaton, 1991).

In Figure 7, turbulent Schmidt numbers are presented for the different migration velocities.

Particle Transport in Electrostatic Precipitators

Dispersion coefficient

On the basis of the results presented in the previous section, a model for the dispersion coefficient was induced for the range of particle dimension and migration velocity reported in Table 2. We propose the following model for the turbulent Schmidt number:

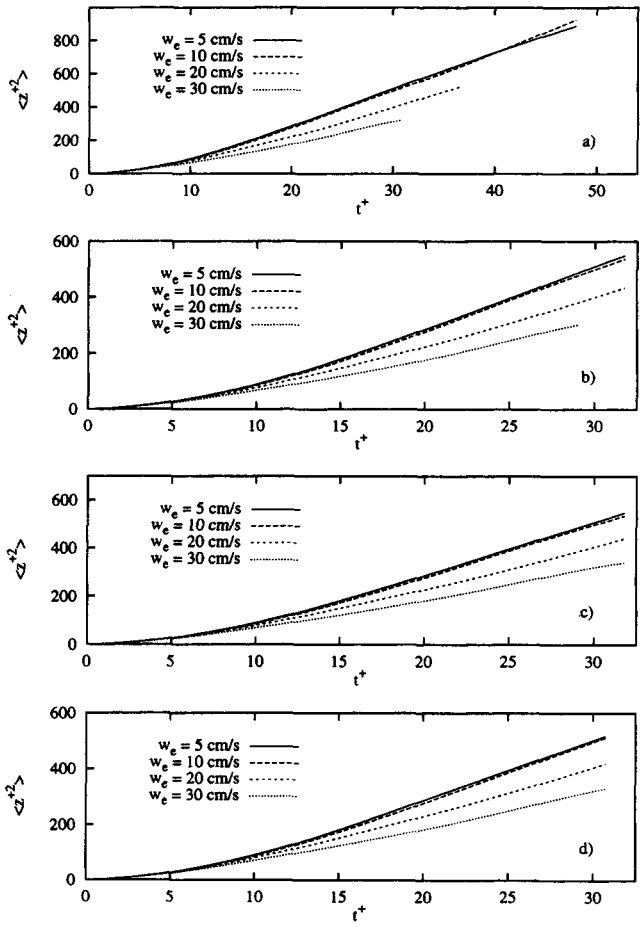

Figure 6. Effect of migration velocity on $\langle z(t)^2 \rangle$: (a) $d_p = 4$ μm; (b) $d_p = 8$ μm; (c) $d_p = 16$ μm; (d) $d_p = 24$ μm.

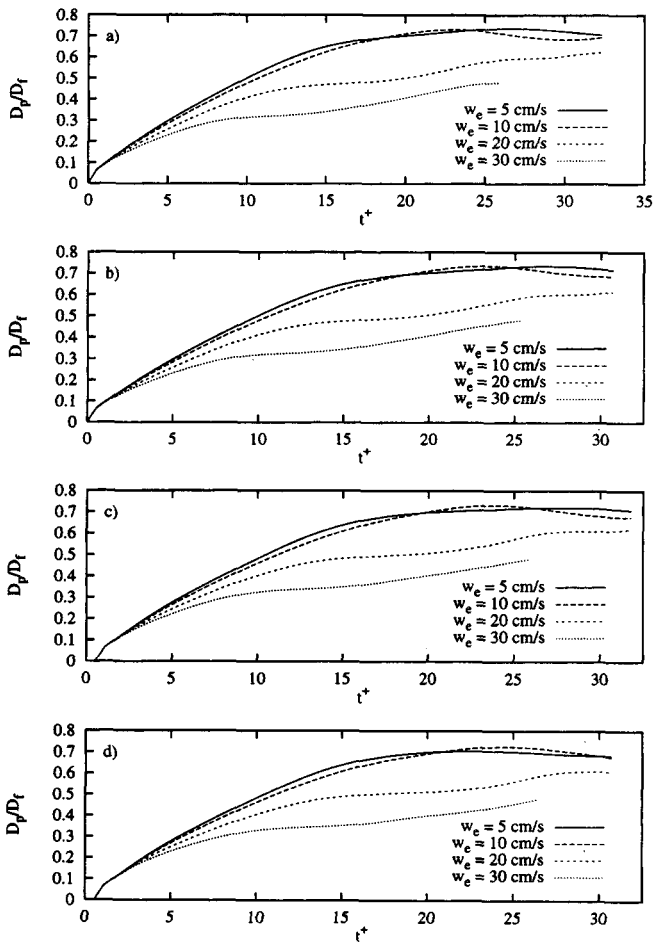

Figure 7. Effect of migration velocity on turbulent diffusivity: (a) $d_p = 4$ μm; (b) $d_p = 8$ μm; (c) $d_p = 16$ μm; (d) $d_p = 24$ μm.

$$Sc_t = \frac{A}{1 + B\tau_p^+} + C, \tag{16}$$

where A, B, and C are functions of the dimensionless migration velocity, $w^* = w_e/\overline{w'}$, and are given by

$$A = 0.25 \exp[-0.55w^*]; \quad B = 7.5w^* + 18.3;$$

$$C = 0.3 \frac{w^* + 69.8}{w^{*2} + 29.4}. \tag{17}$$

The dependence on τ_p^+ is rather weak compared, for example, to the dependence on the drift velocity. However, the dependence on τ_p^+ was considered in order to cover low drift-velocity ranges. Equation 16 was obtained by fitting the numerical database obtained in this work. The comparison is shown in Figure 8, which contains all the results related to the determination of the diffusion coefficients.

On examining Figure 7, it is evident that a constant asymptotic value for the Schmidt number is not obtained for particles with higher migration velocity. In such cases, the diffusion coefficients were computed through a fit of the displacement variance curves (Figure 6) in the linear region, that is, for times longer than the Lagrangian autocorrelation time.

In order to compare the results of Eq. 16 with other sources, a review was made of the existing literature. It was seen that most of the numerical computations and models for diffusion of particles in homogeneous turbulence (Squires and Eaton, 1991; Yeh and Lei, 1991; Elgobashi and Truesdell, 1992; Wang and Stock, 1993, among others) were assessed against the experimental data by Wells and Stock (1983), and against the theory proposed by Csanady (1963). Wells and Stock (1983) obtained their data in a model electrostatic precipitator model with the object of examining the effect of crossing

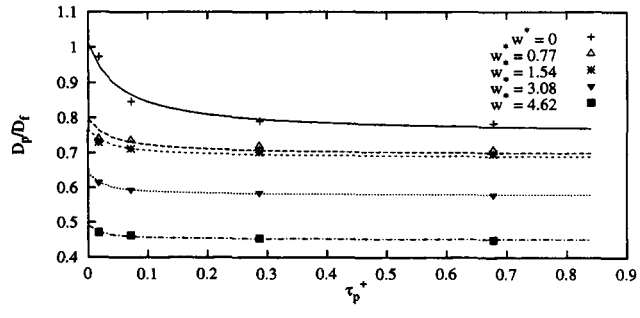

Figure 8. Computed diffusivity (symbols) and proposed correlation (lines).

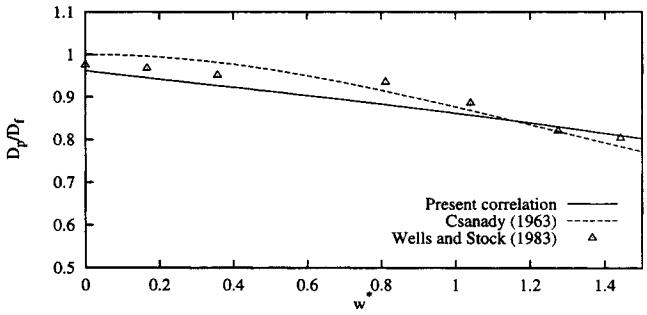

Figure 9. Behavior of the turbulent diffusion coefficient vs. dimensionless migration velocity.

Comparison of present correlation experimental data by Wells and Stock (1983) and equation of Csanady (1963).

trajectories on particle dispersion. They used a grid to break turbulence structures and to obtain a roughly homogeneous flow field. They used particles of 5 and 57 μm and varied the electrostatic charge. Csanady (1963) proposed models to calculate longitudinal and transverse turbulent diffusion coefficients for particles in homogeneous turbulence. The expression for the transverse turbulent Schmidt number is

$$\frac{D_p}{D_f} = Sc_t = \left[1 + \frac{4\beta^2 w_e^2}{\overline{w'}^2}\right]^{1/2}, \qquad (18)$$

where $\beta = \overline{w'} T_L / L_E$, in which T_L is the Lagrangian integral time scale and L_E is the Eulerian integral length scale. In their work, Wells and Stock (1983) compared their data with predictions of Eq. 18 and, from their experiments, obtained $4\beta = 0.55$. They also measured values for $\overline{w'}$, which, since the homogeneous turbulence was grid generated, was decaying. Thus, particles were exposed to a decreasing turbulence intensity. A mean value of $\overline{w'}/U_m = 2.5\%$ was estimated and used in Eq. 16. The data of Wells and Stock (1983) in the range of parameters of interest are presented together with predictions by Eq. 16 and the model of Csanady (1963). The present correlation (Eq. 17) compares well both with data by Wells and Stock (1963) and with the model proposed by Csanady (1963), in the range of parameters examined.

The agreement between the present correlation and the other sources suggests that the hypothesis of nearly homogeneous dispersion, on the basis of which the diffusion coefficients were calculated in this work, is acceptable for many purposes. Furthermore, the agreement of Eq. 16 with the model by Csanady (1963), at least for the range of values presented in Figure 9, indicates that they may be used interchangeably to calculate the diffusion coefficient in the transverse direction. The use of the relation given by Csanady (1963) requires that both a Lagrangian integral time scale and an Eulerian integral length scale be known, while the use of Eq. 16 requires just that the average value of the turbulent cross-stream velocity fluctuations be known, and is therefore more convenient from a practical viewpoint.

Collection efficiency in plate – plate electrostatic precipitators

The most important design parameter for ESPs is the collection efficiency. As previously discussed, Eq. 1 is based on assumptions that are not easy to justify. Yet, even in recent contributions (Riehle and Löffler, 1992), it is considered a suitable tool to interpret precipitation mechanisms. Equation 1 significantly underpredicts deposition rates when applied to controlled laboratory experiments. As an aside, to improve the efficiency of industrial precipitators, it is necessary to isolate the various mechanisms that cause performance to deteriorate in comparison to more ideal systems. This requires, as a first step, reasonable predictions of the turbulence effect on particle dispersions and advection.

Table 3. Parameters Relative to the Simulation of Particle Dispersion and Collection Efficiency

τ_p^+	Fr_p	d_p^+	d_p (m)	E (V/m)	q (C)	w_e (cm/s)
0.018	0.18	0.022	4×10^{-6}	2.39×10^{5}	1.60×10^{-16}	5
0.072	0.25	0.043	8×10^{-6}	2.39×10^{5}	6.39×10^{-16}	10
0.286	0.36	0.086	16×10^{-6}	2.39×10^{5}	2.55×10^{-15}	20
0.645	0.44	0.129	24×10^{-6}	2.39×10^{5}	5.74×10^{-15}	30

The analysis of turbulence effects on collection efficiency was performed by simulating different swarms of particles: each swarm comprised 4,000 particles that were initially distributed homogeneously in the duct, a condition similar to that occurring in real ESPs. The parameters characterizing particles are reported in Table 3.

In Figure 10, the (computed) fractional concentration profiles are reported for different Deutsch numbers, and compared with experimental data from Kihm (1987), and show good agreement. The effect of finite diffusivity on the concentration profile, which, according to the theory by Deutsch, would be uniform across the duct, is also evident. As the collection process goes on, particle concentration decreases in the bulk-flow region, but remains constant in the region near the collecting wall. If the drift velocity of depositing particles were constant, the number of particles collected at different downstream locations should be a linear function of the stream-wise coordinate. This behavior is observed in Figure 11, where efficiencies computed for the cases reported in Table 3 are presented as a function of the downstream coordinate x. For all curves, a linear increase in the efficiency occurs up to a certain value, which decreases with particle size (and, in turn, particle drift), followed by an asymptotic, Deutsch-like behavior. The linear rise can be explained using a plug-flow model (which, in the literature, is incorrectly referred to as a laminar flow model, e.g., Leonard et al., 1980), in which particles drift toward the collecting wall at a con-

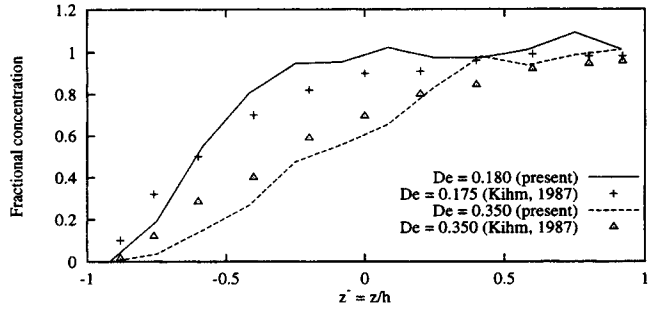

Figure 10. Particles concentration profiles across the channel.

Comparison of present computations against data by Kihm (1987).

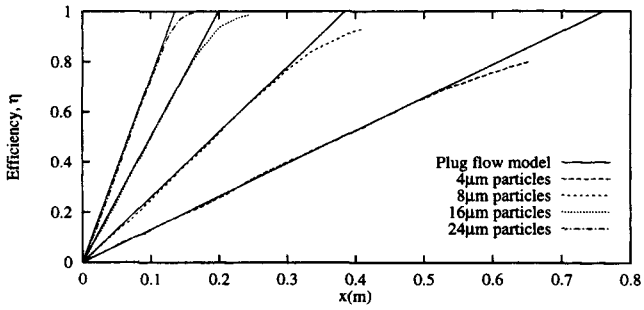

Figure 11. Collection efficiency vs. downstream distance of present simulations.

Comparison with a plug-flow model.

stant, effective migration velocity, w_{eff}, and move downstream with a uniform velocity profile, which may be assumed to be the same as the mean velocity of the fluid, U_m. According to this model, the efficiency is

$$\eta = \frac{w_{\text{eff}} x}{U_m 2h} = De_{\text{eff}}, \tag{19}$$

which predicts that all particles will be collected for a Deutsch number equal to one. In Figure 11, the linear part of the efficiency curves was fitted in order to obtain a value for the effective migration velocity of the model. In this way, values of 4.6, 9.2, 17.8 and 26.3 cm/s for w_{eff}, for particle diameters of 4, 8, 16 and 24 μm, respectively, were obtained. These values are lower than w_e (see Table 3). However, if the actual migration velocity, w_a, of the suspended particles is calculated, the values 4.56, 9.15, 17.6 and 26.1 cm/s are obtained for particle diameters of 4, 8, 16 and 24 μm. This indicates that the early stages of collection are well predicted by a plug-flow model if the actual value of the migration velocity is used.

The simple plug-flow model is not adequate to predict the behavior of the collection efficiency for later stages. In this case, a two-dimensional ADE can be used in the form

$$U_m \frac{\partial n}{\partial x} + w_a \frac{\partial n}{\partial z} - D\left(\frac{\partial^2 n}{\partial x^2} + \frac{\partial^2 n}{\partial z^2}\right) = 0, \tag{20}$$

where the convection term has been expressed in the Fickian form. The flux of particles that are deposited at the wall is given by $n^* \cdot w$. Here, n^* is the concentration of particles in the fluid layer immediately facing the wall, and w is the velocity of particles along z. From Eq. 20, the volumetric flux, that is, the depositing velocity, is

$$w = w_a - \frac{D}{n}\frac{\partial n}{\partial z}. \tag{21}$$

In the early stages of deposition, the gradient of the concentration at the wall is zero (see also Figure 10), the depositing flux is constant, and the efficiency rises linearly. When the number of suspended particles is smaller, the gradient of the concentration profiles at the wall has a finite, increasing value, the depositing flux starts decreasing, and the slope of the efficiency curve keeps decreasing with the streamwise coordinate. In Figure 12, the deposition efficiency for the four cases

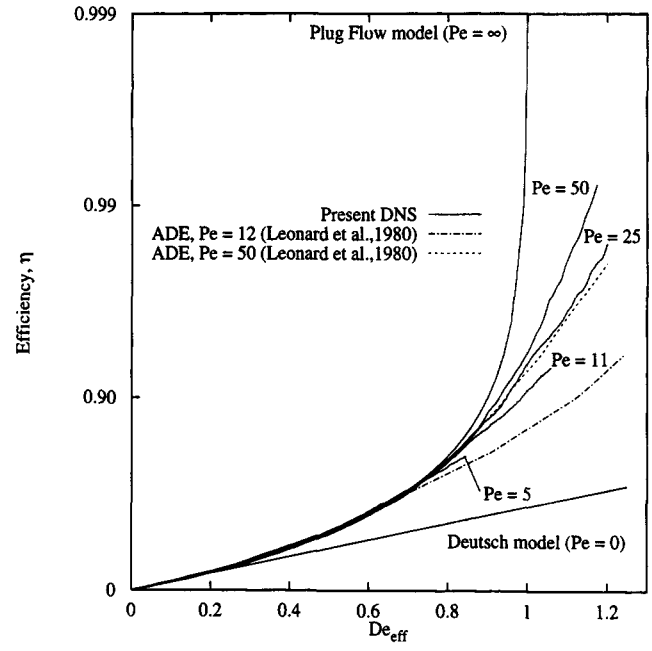

Figure 12. Collection efficiency vs. effective Deutsch number.

Comparison of present simulations with the plug-flow model, Deutsch model, and numerical solution of a 2-D ADE of Leonard et al. (1980).

of Table 3 is plotted against the effective Deutsch number. The lines of the numerically simulated cases lie in between the two extreme cases: the Deutsch model, which implies turbulent diffusion-dominated particle transport, and the plug-flow model, in which turbulent diffusion has no role. The Péclet numbers reported in Figure 12 have been calculated using the actual migration velocity. The numerical solution of Eq. 20 given by Leonard et al. (1980), who used a finite difference method in place of the less practical analytical solution in the form of a series expansion, is also plotted in Figure 12. At the collecting wall, since turbulent diffusivity goes to zero at the wall, Leonard et al. (1980) employed the boundary condition

$$k\frac{\partial n}{\partial z} + n = 0 \tag{22}$$

at a distance ϵ tending to zero from the collecting wall, with the constant k determined on the basis of physical considerations. The solution found by Leonard et al. (1980), calculated for $Pe = 50$ and $Pe = 12$, is presented in Figure 12: these curves underpredict present simulations relative to the cases $Pe = 50$ and $Pe = 11$ by about 1 to 2%. This effect may be due to the overestimation of the turbulent dispersion effects in the wall layer arising from use of a uniform turbulent diffusion coefficient evaluated in the central region of the duct, where turbulent diffusion is stronger.

Conclusions

An investigation on the effect of transport parameters on particle correlation efficiency in ESP has been performed using a DNS database for turbulent flow in a channel. The flow

field was previously obtained by solving the 3-D time-varying Navier–Stokes equations with a pseudospectral method.

Particle motion in an ESP is dominated by drift velocity and turbulent dispersion. An analysis of particle transport characteristics was performed by following the motion of different swarms of particles characterized by different diameters and different migration velocities. The effect of such parameters on particle dispersion was determined and a correlation for the turbulent Schmidt number (i.e., the ratio of turbulent particle diffusivity to fluid diffusivity), based on particle characteristic time and drift velocity, was proposed. In principle, since the turbulent flow field is not homogeneous, turbulent diffusion is a function of position. However, following an approach that gave reasonably good results in terms of macroscopic behavior, the diffusion coefficient was determined using the approach proposed by Taylor (1921) for diffusion in homogeneous turbulence. The proposed correlation, fitted to DNS data, was assessed vis à vis experimental data (Wells and Stock, 1983) and theory (Csanady, 1963). It gave good results in the range of parameters examined. It may be used interchangeably with the model proposed by Csanady (1963), but is more convenient for many purposes.

The usual approach for determining collection efficiency follows the solution of the 2-D ADE in terms of unknown values of the diffusion coefficient. In this work, accurate values of the bulk-diffusion coefficient and of the actual migration velocity of particles were determined and used to verify the adequacy of simplified models. Collection efficiencies were examined for different classes of particles. It was found that the early stages of the collection process may be interpreted with the plug-flow model: on this basis, the flux of depositing particles is given by multiplying particle concentration in the wall region, which is constant, by the actual migration velocity. The plug-flow model fails when the number of airborne particles decreases below a certain value, sufficient to modify the concentration profile at the wall. From this crossover point on, particle collection is controlled by turbulent bulk-dispersion mechanisms. For smaller particles, this crossover point is found to occur at earlier stages, because their transport is more influenced by turbulent diffusion. The interpretation of particle-collection behavior in the later stages requires the use of a 2-D advection diffusion equation at least. It is shown that if the actual values of turbulent diffusion and migration velocity are used, that is, values calculated from the present simulations, predictions of the ADE underestimate the present simulations by about 1%. One cause of this discrepancy may be related to the use of a uniform diffusion coefficient that is representative of turbulent diffusion in the central region of the channel, but overestimates turbulent transport in the wall layers.

Acknowledgments

This work was supported by CNR under grant 94.01726.CT03. Computational resources provided by CINECA Supercomputing Center, Casalecchio di Reno (BO), Italy, under grant C92-T2TUDZP1 on CRAY C92/2128, are gratefully acknowledged. Contract N00014-92-J10774 supported the development of the kernel of the pseudospectral code.

Literature Cited

Aggarwal, S. K., Y. Xiao, and J. Uthuppan, "Effect of Stokes Number on Particle Dispersion," *At. Sprays*, **4**, 223 (1994).

Batchelor, G. K., "Diffusion in Free Turbulent Shear Flows," *J. Fluid Mech.*, **3**, 67 (1957).

Chein, R., and J. N. Chung, "Simulation of Particle Dispersion in a Two-Dimensional Mixing Layer," *AIChE J.*, **34**, 946 (1988).

Chen, M., and J. B. McLaughlin, "A New Correlation for the Aerosol Deposition Rate in Vertical Ducts," *J. Colloid Interf. Sci.*, **169**, 437 (1995).

Cooperman, P., "A New Theory of Precipitator Efficiency," *Atmos. Environ.*, **5**, 541 (1971).

Cooperman, P., "Efficiency Theory and Practice in Electrostatic Precipitation," *Proc. Fourth Int. Clean Air Congr.*, Tokyo, **46**, p. 835 (1977).

Cooperman, P., "Particle Transport in Electrostatic Precipitators—Discussion," *Atmos. Environ.*, **16**, 1568 (1982).

Crowe, C. T., J. N. Chung, and T. R. Troutt, "Particle Mixing in a Free Shear Flow," *Prog. Energy Combust. Sci.*, **14**, 171 (1988).

Csanady, G. T., "Turbulent Diffusion of Heavy Particles in the Atmosphere," *J. Atmos. Sci.*, **20**, 201 (1963).

Deutsch, W., "Bewegung und Ladung der Elektrizititätsträger in Zylinder Kondensator," *Ann. Phys.*, **58**, 335 (1922).

Elghobashi, S., and G. C. Truesdell, "Direct Simulation of Particle Dispersion in a Decaying Isotropic Turbulence," *J. Fluid Mech.*, **242**, 655 (1992).

Kim, J., P. Moin, and R. Moser, "The Turbulence Statistics in Fully Developed Channel Flow at Low Reynolds Number," *J. Fluid Mech.*, **177**, 133 (1987).

Kihm, K. D., "Effects of Nonuniformities on Particle Transport in Electrostatic Precipitators," PhD Diss., Dept. of Mechanical Engineering, Stanford Univ., Stanford, CA (1987).

Kontomaris, K., and T. J. Hanratty, "Effect of Molecular Diffusivity on Point Source Diffusion in the Centre of a Numerically Simulated Turbulent Channel Flow," *Int. J. Heat Mass Transfer*, **37**, 1817 (1994).

Lam, K., and S. Banerjee, "On the Condition of Streak Formation in Bounded Flows," *Phys. Fluids A*, **4**, 1289 (1992).

Leonard, G. L., M. Mitchner, and S. A. Self, "Particle Transport in Electrostatic Precipitators," *Atmos. Environ.*, **14**, 1289 (1980).

Leonard, G. L., M. Mitchner, and S. A. Self, "Experimental Study of the Effect of Turbulent Diffusion on Precipitator Efficiency," *J. Aerosol Sci.*, **13**, 271 (1982).

Meek, C. C., and B. G. Jones, "Studies of the Behavior of Heavy Particles in a Turbulent Fluid Flow," *J. Atmos. Sci.*, **30**, 239 (1973).

Nir, A., and L. M. Pismen, "The Effect of a Steady Drift on the Dispersion of a Particle in Turbulent Fluid," *J. Fluid Mech.*, **94**, 369 (1979).

Ounis, H. G., G. Ahmadi, and J. B. McLaughlin, "Dispersion and Deposition of Brownian Particles from Point Sources in a Simulated Turbulent Channel Flow," *J. Colloid Interf. Sci.*, **147**, 233 (1991).

Papavassiliou, D. V., and T. J. Hanratty, "The Use of Lagrangian Methods to Describe Turbulent Transport of Heat from a Wall," *Ind Eng. Chem. Res.*, **34**, 3359 (1995).

Pismen, L. M., and A. Nir, "On the Motion of Suspended Particles in Stationary Homogeneous Turbulence," *J. Fluid Mech.*, **84**, 193 (1978).

Reeks, M. W., "On the Dispersion of Small Particles Suspended in an Isotropic Turbulent Field," *J. Fluid Mech.*, **83**, 529 (1977).

Reynolds, A. M., "The Relative Dispersion of Particles in Isotropic Homogeneous Turbulence," *Fluid Dyn. Res.*, **16**, 1 (1995).

Riehle, C., and F. Löffler, "The Effective Migration Rate in Electrostatic Precipitators," *Aerosol Sci. Technol.*, **16**, 1 (1992).

Robinson, M., "A Modified Deutsch Efficiency Equation for Electrostatic Precipitation," *Atmos. Environ.*, **1**, 193 (1967).

Rowe, P. N., and G. A. Henwood, "Drag Forces in Hydraulic Model of a Fluidized Bed-Part I," *Trans. Instn. Chem. Engrs.*, **39**, 43 (1962).

Self, S. A., K. D. Kihm, and M. Mitehner, "Precipitator Performance Improvement through Turbulence Control," *Proc. Third Int. Conf. Electrostatic Precipitation*, Abano, Italy, p. 443 (1987).

Soldati, A., P. Andreussi, and S. Banerjee, "Direct Simulation of Turbulent Particle Transport in Electrostatic Precipitators," *AIChE J.*, **39**, 1910 (1993).

Soldati, A., P. Andreussi, and S. Banerjee, "Direct Simulation of Turbulent Particle Transport in Electrostatic Precipitators—Reply," *AIChE J.*, **41**, 739 (1995a).

Soldati, A., P. Andreussi, and S. Banerjee, "Direct Numerical Simu-

lation of Turbulent Dispersion Under Steady Drift," *Chaos and Fractals in Chemical Engineering*, G. Biardi, M. Giona, and A. R. Giona, eds., World Science, Singapore, p. 105 (1995b).
Squires, K. D., and J. K. Eaton, "Measurements of Particle Dispersion Obtained from Direct Numerical Simulation of Isotropic Turbulence," *J. Fluid Mech.*, **226,** 1 (1991).
Taylor, G. I., "Diffusion by Continuous Movements," *Proc. Lond. Math. Soc.*, **20,** 196 (1921).
Tsai, R., "A Study of the Effect of Turbulence on Electrostatic Precipitator Performance," PhD Thesis, Univ. of California, Los Angeles (1991).
Wang, L. P., and D. E. Stock, "Dispersion of Heavy Particles by Turbulent Motion," *J. Atmos. Sci.*, **13,** 1897 (1993).
Wells, M. R., and D. E. Stock, "The Effect of Cross Trajectories on the Dispersion of Particles in a Turbulent Flow," *J. Fluid Mech.*, **136,** 31 (1983).
Williams, J. C., and R. Jackson, "The Motion of Solid Particles in an Electrostatic Precipitator," *Proc. Symp. Interaction Between Fluids and Particles, Trans. Inst. Chem. Engrs.*, London, p. 282 (1962).
Yeh, F., and U. Lei, "On the Motion of Small Particles in a Homogeneous Turbulent Shear Flow," *Phys. Fluids*, **3**, 2758 (1991).
Yeung, P. K., and S. B. Pope, "An Algorithm for Tracking Fluid Particles in Numerical Simulations of Homogeneous Turbulence," *J. Comput. Phys.*, **79,** 373 (1988).
Yudine, M. I., "Physical Considerations on Heavy-Particles Diffusion: Atmospheric Diffusion and Air Pollution," *Adv. Geophys.*, **6,** 185 (1959).

Manuscript received July 24, 1996, and revision received Dec. 4, 1996.